Analysis of Multi-Scale Energy Markets using Stochatic Optimization Techniques

ISyE 719 Course Project

Apoorva Sampat and Ranjeet Kumar
Department of Chemical and Biological Engineering
University of Wisconsin, 1415 Engineering Dr, Madison, WI 53706, USA

Abstract

Electricity markets operate at multiple timescales (from hours to milliseconds) to ensure that supply and demands are matched in real time. These markets involve uncertainties because future electricity prices and demands are unknown at the time of decision-making, e.g. energy sale and purchase commitments by generators. We use stochastic programming techniques to study flexibility and economic opportunities provided by a battery in these markets, namely day-ahead (1-hour timescale) and real-time (5-minute timescale) markets. In this work we consider uncertainty only in electricity loads and determine optimal participation strategies using methods like receding horizon scheme, dual dynamic programming and *fullproblem (scenario sampling)*. We also determine bounds on expected policy costs by using perfect information and two-stage approximation (with restriction on states). We compare the costs of participation in exclusively in day-ahead market and both day-ahead and real-time markets. Our results show that market participation only in day-ahead energy markets can *significantly* reduce economic flexibility as compared to participating in both levels of markets.

1 Introduction

A diverse set of energy systems such as generators, batteries, wind turbines and flywheels can participate in electricity markets. This participation is governed by rules set by ISOs (Independent System Operators) such as California ISO, PJM (Pennsylvania-New Jersey-Maryland) Interconnection and Midcontinent ISO, under whose jurisdiction the market falls. The markets are structured at multiple time levels, namely day ahead (hourly market commitments) and real time markets (commitments ranging from minutes to seconds). In day-ahead markets the electricity is traded in intervals of 1 hour with the prices being constant in each interval of 1 hour and varying with intervals. Real time markets, on the other hand can have varying time scales depending on the ISO operating it. The frequency of energy price variation is different for day-ahead and real time markets (Figure 1).

Apart from price variations, the introduction of more renewable power sources in the grid such as wind and solar energy, there are greater variations and uncertainties in the net load as well. Since these sources depend on intermittent conditions such as weather, they introduce slow dynamics to

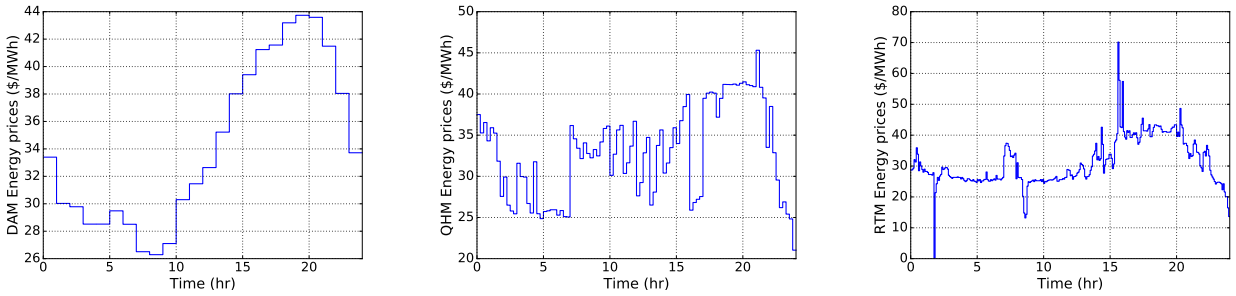

(a) Day-ahead market (b) Quarter-hourly market (c) Real-time market

Figure 1: Energy prices for one day in the markets in California

the grid. Thus systems with faster dynamic responses such as battery and building systems are becoming increasingly important to balance these fluctuations and provide dynamic flexibility to the power grid. Also, factors such as transmission losses, generation cost and congestion affect the value of products (energy, regulation, spinning , non-spinning reserves) offered at different timescales. These fluctuations being inherently uncertain, determining the optimal participation policy requires analysis using stochastic optimization techniques.

2 Problem Definition and Decision-Making Setting

We consider a rechargeable Li-ion battery with a building that is inter-connected to the power grid for providing electricity services. Electricity services imply that batteries can provide power to or draw power from the grid. In our current setting, we do not consider participation in regulation or other ancillary services. The operator of the power grid (ISO) compensates the battery-owners for the electricity services provided. The goal for the battery-owners is to maximize the revenues generated by providing services to the grid and at the same time meeting the load demands from building. Any unmet load demand from the building is penalized.

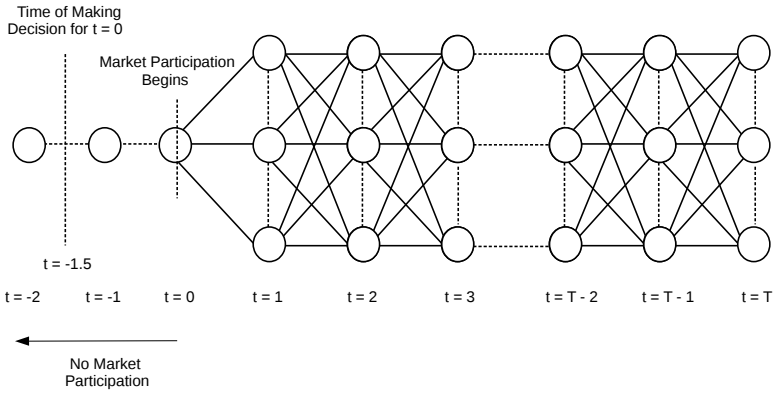

Figure 2: Scenario tree at the beginning of market participation

We divide an annual dataset for electricity loads (available over 5-minute intervals) into 52 subsets of weekly load profiles, i.e 2016 intervals of 5-minute each. This division of data helps in capturing the different load profiles over the weekdays and the weekend. We then use these 52 weekly profiles to generate sample scenarios for our computational experiments (Section 4). Since the loads are correlated between time intervals, we formulate a multivariate normal distribution for weekly loads using a mean vector and a covariance matrix. The mean vector (of size 2016 x 1) is the mean of the 52 datasets, but the covariance matrix (of size 2016 x 2016) calculated directly from the 52 datasets cannot be used, since its rank can at most be 52. So we use the Ledoit-Wolf Covariance Estimator [1] (to tackle rank deficiency) for estimating a full rank covariance matrix. We generate 50 samples of load profiles (Figure 3) for a week using the mean and covariance matrix obtained.

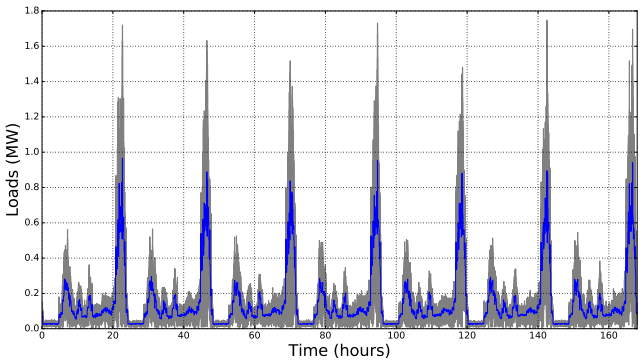

Figure 3: Load scenarios for a week

Cosidering the price data for a full year to be known (deterministic) we can solve the optimization problem to maximize the annual revenues by operating a battery in the power grid for the whole year. In this work, we aim to solve this deterministic optimization problem with two approaches:

1. Simultaneous approach: In this approach, we formulate a single giant optimization problem for a full year and solve it to produce the optimal power and regulation capacities that the battery should operate with in each time interval in all the three markets.

2. Rolling (1 day) horizon approach: In this approach, we formulate an optimization problem for a day and solve it to produce the optimal power and regulation capacities for that day, then take the solutions at the end time-point of that day as the initial point for the next day, then formulate the optimization problem for the next day with those initial values and solve for the second day and sequentially we solve for the 365 days. It is called rolling horizon because in this approach we consider a horizon of 1 day and keep shifting the horizon to to the next day after solving the current day.

At the end, we will compare the two solutions and investigate the advantages and disadvantages of the two approaches.

Understanding the economic incentives provided by generation and load flexibility requires of careful consideration of wholesale electricity market structures and diverse products. Figure **??**

shows the multiscale control structure currently used to balance the power grid. Resources can participate by buying/selling electrical energy and/or providing ancillary services (regulation, reserves). Figure **??** shows time-varying prices from the California Independent System Operator (CAISO) for three consecutive days. Energy is transacted at three timescales: in the integrated forward market (day-ahead market with 1-hour intervals), in the fifteen minute market, and through the real-time dispatch process (5-minute intervals). Table **??** lists the different products transacted at each timescale. Histograms for energy prices at different markets are presented in Figure **??**. As can be seen, prices are less volatile in the day-ahead market and the average price is higher. In the real-time market (FMM, RTD) prices are frequently negative and occasionally exceed \$150/MWh. Energy systems with fast dynamics (e.g., flywheels, batteries) can exploit these fast price fluctuations.

In the U.S., generators/loads provide the hierarchical market structure with addition flexibility via *regulation* and *reserve* ancillary service products.

3 Optimization Model for Battery Systems

3.1 Perfect Information Setting

3.2 Optimization Under Uncertainty

4 Computational Experiments

List of figures

4.1 Full Problem

In this case study, we sample 50 scenario paths for the full week.

- Supplied and unmet load for a sample path
- Prtm
- Pdam
- SOC
- Net discharge
- revenue from energy

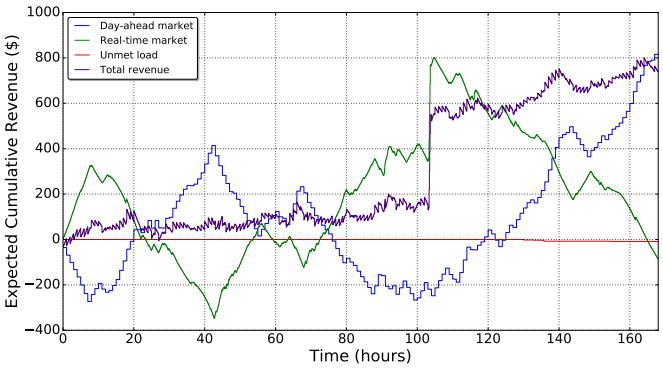

Figure 4: Trajectory of cumulative revenues

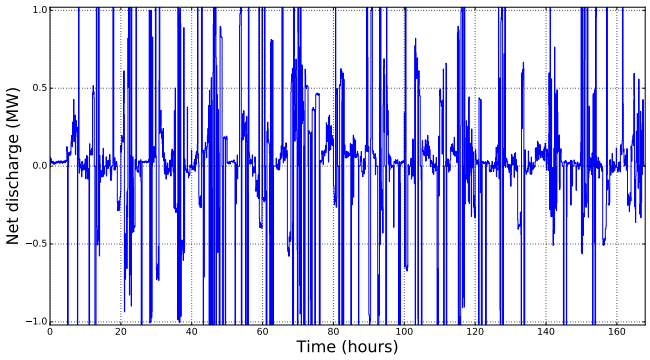

Figure 5: Net battery discharge

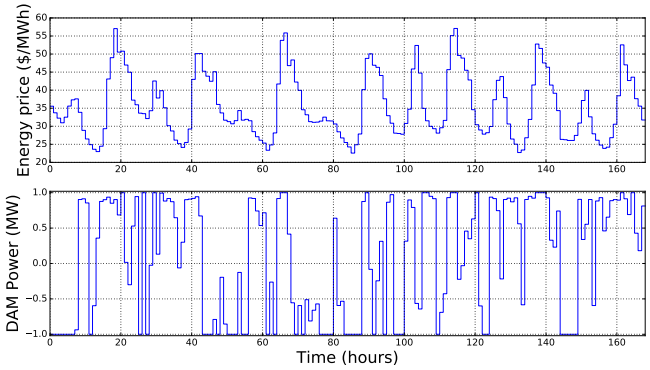

Figure 6: Energy participation policy in day-ahead market

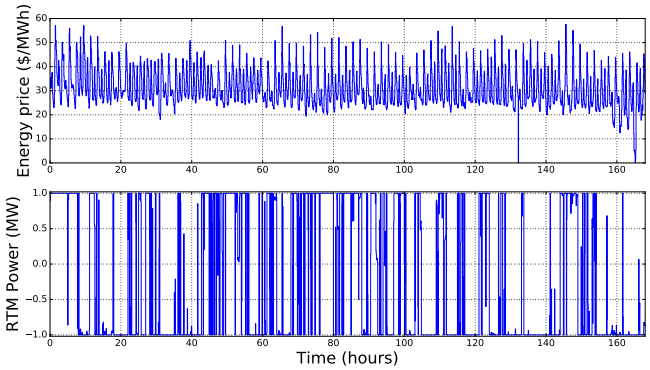

Figure 7: Energy participation policy in real-time market

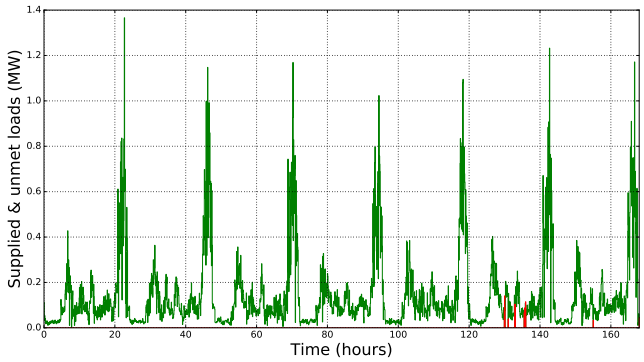

Figure 8: Power supplied to building and unmet load

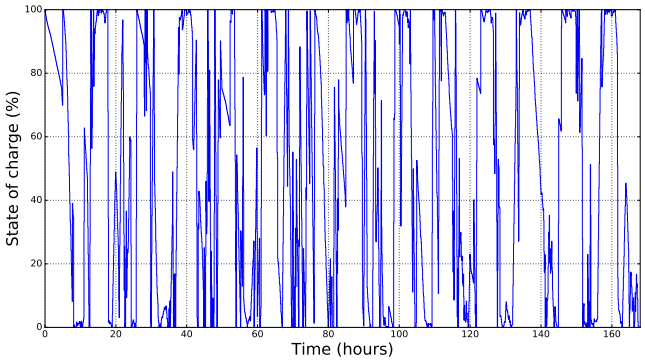

Figure 9: Trajectory of the state of charge of battery

4.1.1 Upper Bound from Mean Value Problem

4.1.2 Estimating Bounds with Perfect Information

4.1.3 Estimating Bounds with Two-Stage Approximation: Restriction

4.2 Receding Horizon Heuristic

We sample 50 paths upto next 24 hours horizon

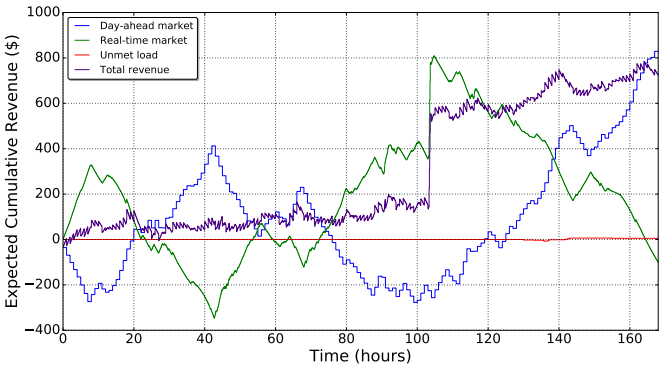

Figure 10: Trajectory of cumulative revenues

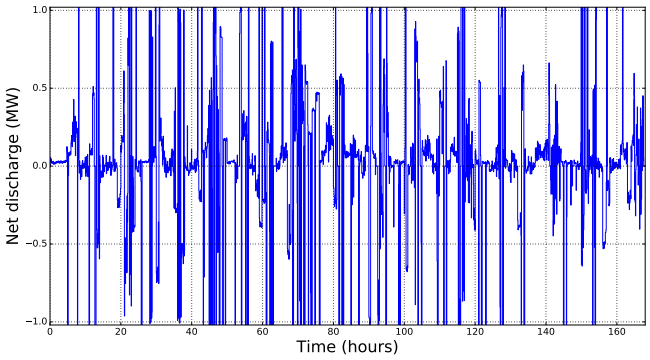

Figure 11: Net battery discharge

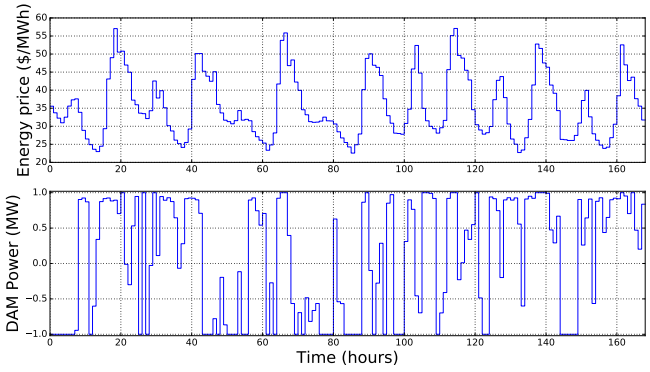

Figure 12: Energy participation policy in day-ahead market

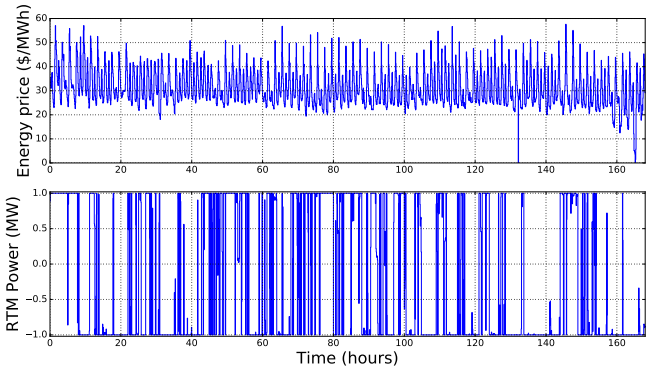

Figure 13: Energy participation policy in real-time market

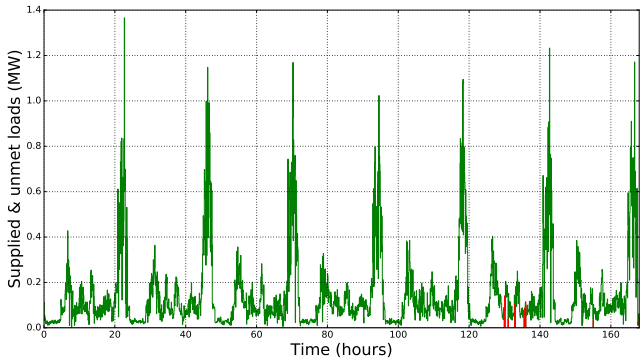

Figure 14: Power supplied to building and unmet load

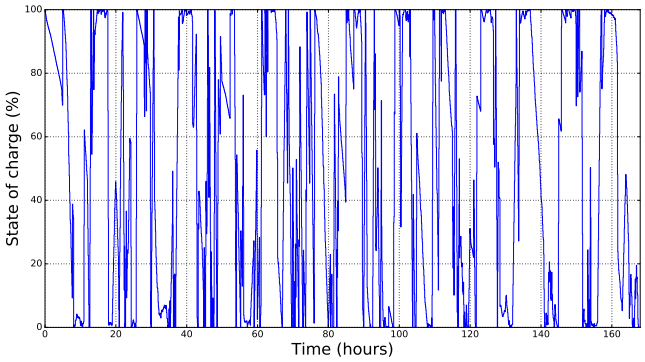

Figure 15: Trajectory of the state of charge of battery

4.3 Stochastic Dual Dynamic Programming

5 Conclusions

6 Future Work

6.1 Price Uncertainty

6.2 Three Layer Markets

we have used for previous studies [4]. The system comprises 2,522 lines, 1,908 nodes, 870 demands points, and 225 generators points (153 gas-fired generators). Because of the difficulty in obtaining natural gas infrastructure data, we construct a simulated natural gas network system using the basic topology reported by the EIA (see http://www.eia.gov/pub/oil_gas/natural_gas/analysis_publications/ngpipeline/midwest.html) and by using engineering insight to ensure gas supply to all the gas-fired power plants under nominal conditions. The gas network designed comprises 215 pipeline segments, 157 nodes, 12 compression stations, and 4 supply points. The resulting network in sketched in Figure **??**.

6.3 Economic Issues

We compare economic performance for the infrastructures under coordinated and uncoordinated settings. We use a time horizon of 24 hours. The results are summarized in Table 1. In our simulations, the electrical loads were always satisfied; consequently, we report only the generation cost component of the grid cost φ^{grid}. From the results we make the following observations:

- Under a coordinated setting the power cost decreases by 0.38% which represents a total of $140,000. The gas cost decreases by 7%, which corresponds to a total of $970,000.
- Under an uncoordinated setting only 96% of the gas requested is delivered. *At a gas price of 3 $/MMBTU (see http://www.eia.gov/naturalgas/weekly/), the total undelivered gas has an economic value of $599,000.*
- Under a coordinated setting the compression cost increases by 17.4%. This is the result of an increased amount of gas delivered to the power plants. In particular, *7% more gas is delivered under the coordinated setting.* At a gas price of 3 $/MMBTU, the value of the additional gas delivered is $1,070,000. Note that the total increase in compression cost is negligible compared to the additional value of the delivered demand.
- Under a coordinated setting the revenue for the gas-fired generators increases by 27%, which corresponds to a total of $800,000. This the result of the additional gas delivered and the decreased revenue penalties resulting from coordination.

Table 1: Economic performance under coordinated and uncoordinated settings (scm= standard cubic meters and M$=million U.S. dollars).

	φ^{grid} [M$]	φ^{gas} [M$]	$\varphi^{gas,comp}$ [$]	$d^{gas,target}$[scm $\times 10^{-6}$]	d^{gas} [scm$\times 10^{-6}$]	$\mathcal{R}$ [M$]
Uncoord	36.54	-13.52	28,618	141.25	135.54	2.70
Coord	36.40	-14.54	33,600	145.74	145.74	3.50

It is rather surprising that both the gas and power grid sides benefit from coordination (i.e., *the objectives of the gas and grid operators do not compete*). Moreover, gas-fired generators increase their revenue. We can explain the decreased performance under an uncoordinated setting from the fact

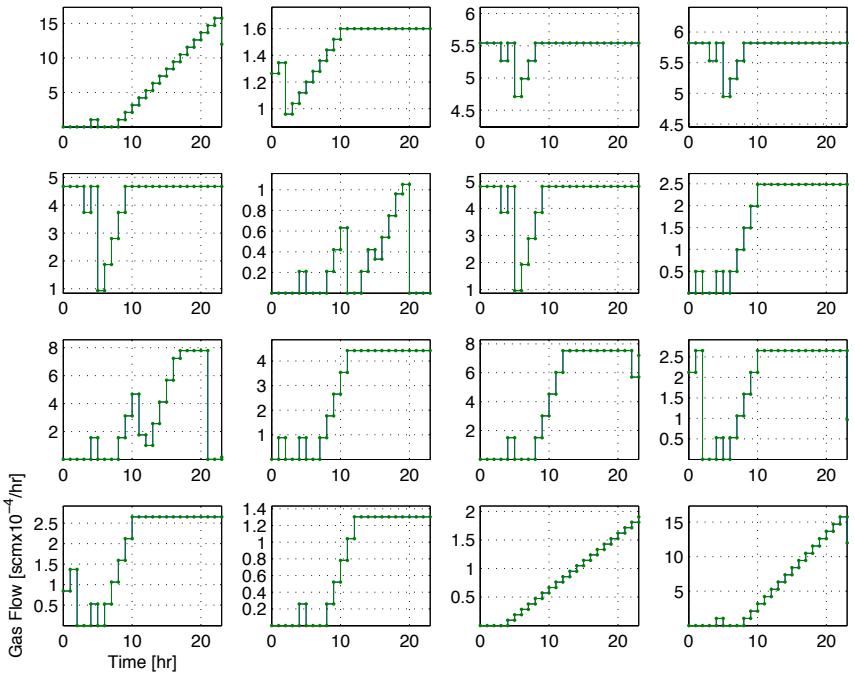

Figure 16: Requested (blue solid line) and realized (green dotted line) gas demands for 16 power plants under coordinated setting.

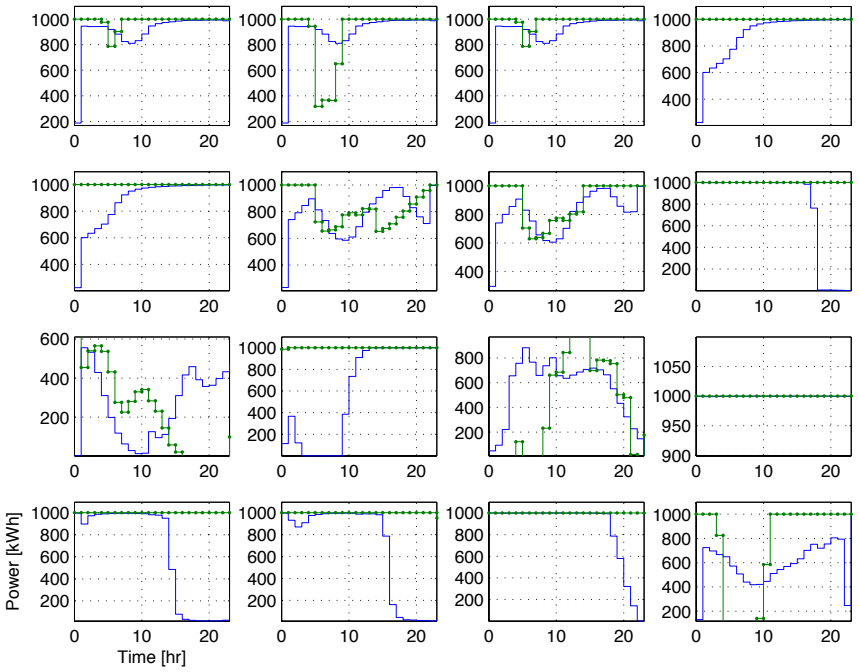

Figure 17: Power compression profiles under uncoordinated (blue) and coordinated (green) settings for 16 different compressor stations.

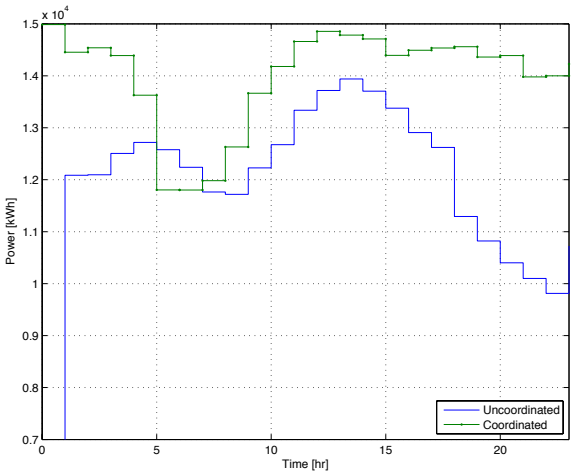

Figure 18: Total compression power uncoordinated (blue) and coordinated (green).

that the power grid operator cannot easily determine how much gas can the gas network deliver at different spatial locations and at different times. Thus, the power grid operator can be overly optimistic (as in the case presented) or pessimistic about the amount of gas that can actually be delivered. This situation is clearly illustrated in Figure **??**, where we present the target and realized gas demands for 16 different gas-fired generators for the uncoordinated setting. Note that the gas network cannot deliver the total amount of gas requested at four locations. The resulting error in the prediction introduces a penalty for both the power grid and the gas-fired generators. In particular, the power grid operator has to dispatch more expensive power plants, resulting in higher a generation cost and the power plants have to pay for the unserved generation. Note also that, *even if the gas operator knows the gas demands of the power grid in advance*, it cannot guarantee to satisfy such demands due to physical constraints. In other words, the spatiotemporal gas demands policies emanating from the power grid dispatch plan can be infeasible to the gas infrastructure.

From Figure **??** we can also see that several gas-fried generators are dispatched aggressively under an uncoordinated setting (i.e., some gas demands are step functions). This is evident from panels 1, 14, 15, and 16 (the panels are numbered row-wise starting from the upper left corner). Line-pack storage in this case is sufficient to track the steep changes in gas demand. Doing so, however, comes at the expense of decreased flexibility at other locations and this leads to unserved demands. From panels 1, 14, 15, and 16 of Figure 16 we also see that dispatch under a coordinated setting is smoother (i.e., demands are ramps) and this significantly enhances the flexibility to deliver gas at other locations. We observe that, under a coordinated setting, gas-fired generators act as *distributed demand response resources* that the gas operator can use to better control network pressures and flows and thus avoid delivery bottlenecks. In other words, *gas-fired power plants become assets rather than liabilities to the pipeline operator.* As a result, all the demand targets can be met and significantly more gas can be delivered compared to the uncoordinated setting. This clearly illustrates the increased physical flexibility gained by coordination.

Figure 17 presents the compression power profiles under coordinated and uncoordinated settings

for 16 different compressor stations. We observe that more compressors operate at full capacity and less variations are observed under a coordinated setting, a situation that is desirable from an efficiency stand-point (i.e., it is inefficient to operate compressors at partial loads and to ramp them up and down continuously from an equipment lifetime and emissions standpoint). From Figure 18 we see that more compression power is used under the coordinated setting because of the increased amounts of gas delivered to the power plants but the compression profile is flatter.

Figures 19 and 20 present axial flow profiles at 16 different pipeline segment for the uncoordinated and coordinated settings, respectively. Each panel presents the time profiles at 10 different axial positions for a given pipeline segment. We can see how the different dispatch plans drastically change the flow profiles of the network. This result indicates that *power grid dispatch decisions can significantly influence the spatiotemporal dynamics of the entire gas infrastructure.*

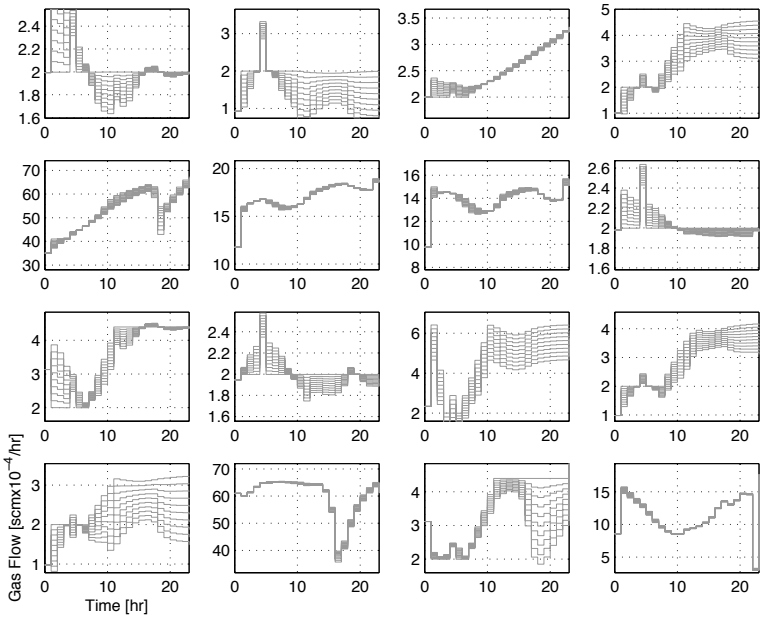

Figure 19: Spatiotemporal flow profiles for 16 different pipeline segments for uncoordinated setting.

6.4 Computational Issues

We now discuss issues related to the implementation and solution of the optimal control model.

6.4.1 Model Implementation

We discretize the continuous-time grid model (**??**) using an implicit Euler discretization scheme. We discretize the gas model (**??**) in time using an implicit Euler scheme and in space using a forward finite-difference scheme. The discretized power grid problem is a linear program, wheres the discretized gas problem is a nonlinear programming problem (NLP). The coupled problem is an NLP. We implement the coupled and decoupled models independently using the algebraic modeling language AMPL. The use of an algebraic modeling language is key because it enables us to obtain exact

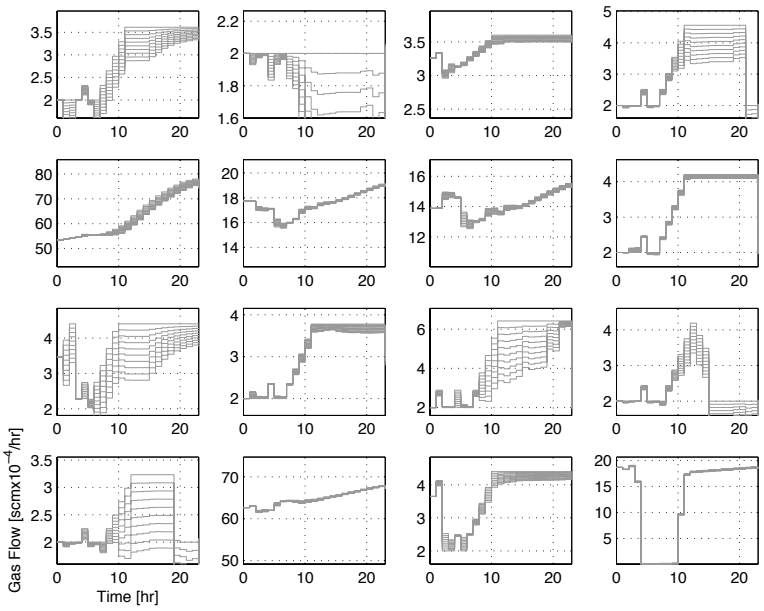

Figure 20: Spatiotemporal flow profiles for 16 different pipeline segments for coordinated setting.

first and second-order derivative information for the gas model. Exact derivatives are essential for efficient handling problems with many degrees of freedom as those arising in interconnected models [3].

6.4.2 Model Solution

We solved the coupled and uncoupled models using a 24-hour time horizon with 1-hour time resolution. In our base implementation we discretize each pipeline segment using $N_x = 10$ finite-difference points. This gives rise to an optimal control problem with 2,400 differential equations, 2000 algebraic equations, and 1040 controls. After full discretization, the coordinated problem (**??**) is an NLP with 249,919 variables, 224,292 equality constraints, and 154,093 inequality constraints. The problem has a total of 25,627 degrees of freedom.

The computational results are summarized in Table 2. The solution time for the base problem is approximately 40 minutes. While the results are acceptable for off-line analysis, such times are too long to consider an actual real-time implementation of the model (which would probably need to be solved every 5 minutes to be compatible with current economic dispatch practices). The long solution times are partially attributed to the high nonlinearity of the gas network model which induces negative curvature. In the presence of negative curvature, the Hessian of the Lagrangian needs to be regularized (convexified) several times during the search and each regularization attempt requires an additional factorization. In particular, in Table 2 we can see that the total number of iterations is 232 while the total number of factorizations is 311, which indicates that 79 regularization attempts are needed.

We also attribute the long solution times to the complexity of the linear algebra system. In partic-

ular, we noticed that MA57 introduced a significant amount of fill-in, an indication of tight connectivity of the algebraic equations. We attribute this to the complexity induced by the PDAEs coupled with the network equations. To confirm this observation, we performed an additional experiment in which we *perturbed the gas network topology by eliminating a single pipeline.* This action splits the Illinois gas network into two independent subnetworks (the power grid topology remains intact). The results for the base and the perturbed topologies are presented in Table 2. The time per iteration is decreased by 18% under the perturbed topology. We also note a significant reduction in the number of iterations and regularizations which indicates that the nonlinearity is ameliorated with a change in topology. In particular, for the base topology we require 311/232=1.34 regularizations per iteration, whereas for the perturbed topology we require 153/136=1.125.

Table 2: Computational results for coupled problems for base and perturbed topologies.

	Iter.	Solution Time [sec]	Factorizations [-]	Time/Factorization [sec]
Base Topology ($N_x = 10$)	232	2401.01	311	7.72
Perturbed Topology ($N_x = 10$)	136	968. 47	153	6.32
Base Topology ($N_x = 3$)	157	573.68	188	3.05

We next analyze the effects of the discretization resolution on the model results. We compare the results using our base implementation with $N_x = 10$ spatial points per pipeline and a low resolution implementation with $N_x = 3$ spatial points per pipeline. This low-resolution problem is an optimal control problem with 2,800 DAEs and 1,040 controls. After full discretization, this gives an NLP with 141,559 variables, 115,932 equality constraints, and 157,765 inequality constraints. The problem has a total of 25,627 degrees of freedom (the number of controls is the same as in the base case). The number of degrees of freedom remains unchanged because all of these enter at the network nodes and are thus independent of the discretization resolution [2]. This is an important structural property of gas networks. The results comparing high and low resolutions are presented in Table 2. The solution time is reduced from 40 minutes to about 10 minutes. Decreasing the resolution decreases both the number of regularizations to 1.19 (compared with 1.34 in the base case) and the time per factorization by a factor 2.5.

We also compare the economic performance of the low- and high-resolution models for the coordinated and uncoordinated settings. The results are presented in Table 3. The amount of compression power in the uncoordinated case is underestimated by 21%, but the impacts on the rest of the metrics are not significant. This indicates that a low discretization resolutions can adequately capture the overall system behavior and can be used to obtain approximate solutions. Despite these improvements, however, we can see that state-of-the-art tools hit their limits of performance on small regional-scale networks and will not be capable of handling ISO-sized domains. Based on the estimates obtained for the Illinois system, we anticipate such NLPs to have tens of millions of variables and constraints. Specialized techniques based on decomposition and adaptive discretizations are needed to address models of this magnitude.

Table 3: Economic performance under low- and high-resolution discretizations.

	φ^{grid} [M$]	φ^{gas} [M$]	$\varphi^{gas,comp}$ [$]	$d^{gas,target}$[scm $\times 10^{-6}$]	d^{gas} [scm$\times 10^{-6}$]	$\mathcal{R}^{gas}$ [M$]
Uncoord ($N_x = 10$)	36.54	-13.52	28,618	141.25	135.54	2.70
Uncoord ($N_x = 3$)	36.51	-13.57	23,592	141.12	135.96	2.74
Coord ($N_x = 10$)	36.40	-14.54	33,600	145.74	145.74	3.50
Coord ($N_x = 3$)	36.39	-14.55	33,356	145.83	145.83	3.48

7 Conclusions

We have presented an optimal control model for integrated gas-electric infrastructures. We used the model to demonstrate that significant improvements in economic performance and flexibility can be gained by coordinated dispatch. Using a large-scale study we demonstrated that, under a coordinated setting, it is possible to deliver significantly larger amounts of gas to the power grid and to improve the revenue of gas-fired plants. We observe that, under a coordinated setting, power plants act as controllable demand response resources that can be used by the gas pipeline operator to better control pressure and flows in space and time. This allows the gas operator to bypass delivery bottlenecks. We also used our model to illustrate that power dispatch policies can strongly influence the flow dynamics of the gas infrastructure. In addition, we found that the state-of-the-art tools can adequately address regional-scale networks but are insufficient to address national-scale networks. As part of future work, we will develop scalable linear algebra strategies based on decomposition and multi-grid techniques to address such problems. We will also develop models that capture transient stability of the power grid and that capture other dependencies between infrastructures. For instance, we will model dual-drive compressors that can run on both natural gas and electricity.

Acknowledgments

This material is based upon work supported by the U.S. Department of Energy, Office of Science, under Contract No. DE-AC02-06CH11357.

References

[1] Olivier Ledoit and Michael Wolf. A well-conditioned estimator for large-dimensional covariance matrices. *Journal of multivariate analysis*, 88(2):365–411, 2004.

[2] Victor M Zavala. Stochastic optimal control model for natural gas networks. *Computers & Chemical Engineering*, 64:103–113, 2014.

[3] Victor M Zavala and Lorenz T Biegler. Nonlinear programming strategies for state estimation and model predictive control. In *Nonlinear model predictive control*, pages 419–432. Springer, 2009.

[4] Victor M Zavala, Audun Botterud, Emil Constantinescu, and Jianhui Wang. Computational and economic limitations of dispatch operations in the next-generation power grid. In *Innovative Technologies for an Efficient and Reliable Electricity Supply (CITRES), 2010 IEEE Conference on*, pages 401–406. IEEE, 2010.